The higher relative concentration of K^+ to Na^+ in saline water improves soil hydraulic conductivity, salt leaching efficiency and structural stability

Sihui Yan [a, b], Tibin Zhang [a, c, *], Binbin Zhang [a, b], Tonggang Zhang [a, b], Yu Cheng [a, b], Chun Wang [a, b], Min Luo [a, b], Hao Feng [a, c], Kadambot H.M. Siddique [d]

[a.] Key Laboratory of Agricultural Soil and Water Engineering in Arid and Semiarid Areas, Ministry of Education, Northwest A&F University, Yangling, Shaanxi 712100, P. R. China

[b.] College of Water Resources and Architecture Engineering, Northwest A&F University, Yangling, Shaanxi 712100, P. R. China

[c.] Institute of Soil and Water Conservation, Northwest A&F University, Yangling, Shaanxi 712100, P. R. China

[d] The UWA Institute of Agriculture, The University of Western Australia, Perth, WA 6001, Australia

* Corresponding author at: Institute of Soil and Water Conservation, Northwest A&F University, Yangling, Shaanxi 712100, China. Tel.: +86 29 87012871; fax: +86 29 87011354. E-mail: zhangtibin@163.com (T. Zhang)

Abstract

Soil salinity and sodicity caused by saline water irrigation are widely observed globally. Clay dispersion and swelling are influenced by sodium (Na^+) concentration and electrical conductivity (EC) of soil solution. Specifically, soil potassium (K^+) also significantly affects soil structural stability, but which concern was rarely addressed in previous studies or irrigation practices. A soil column experiment was carried out to examine the effects of saline water with different relative concentrations of K^+ to Na^+ (K^+/Na^+), including K^+/Na^+ of 0:1 (K0Na1), 1:1 (K1Na1), 1:0 (K1Na0) at a constant EC (4 dS m^{-1}), and deionized water as the control (CK), on soil physicochemical properties. The results indicated that at the constant EC of 4 dS m^{-1}, the infiltration rate and water content were significantly ($P < 0.05$) affected by K^+/Na^+ values, K0Na1, K1Na1 and K1Na0 significantly ($P < 0.05$) reduced saturated hydraulic conductivity by 43.62%, 29.04% and 18.06% respectively compared with CK. The volumetric water content was significantly ($P < 0.05$) higher in K0Na1 than CK at both 15 and 30 cm soil depths. K1Na1 and K1Na0 significantly ($P < 0.05$) reduced the desalination time and required leaching volume. K0Na1 and K1Na1 reached the desalination standard after the fifth and second infiltration, respectively, as K1Na0 did not exceed the bulk electrical conductivity required for desalination prerequisite throughout the whole infiltration cycle at 15 cm soil layer. Furthermore, due to the transformation of macropores into micropores spurred by clay dispersion, soil total porosity in K0Na1 dramatically decreased compared with CK, and K1Na0 even increased the proportion

of soil macropores. The higher relative concentration of K^+ to Na^+ in saline water was more conducive to soil aggregates stability, alleviating the risk of macropores reduction caused by sodicity.

Keywords: Saline water; Cation composition; Hydraulic properties; Desalination; Pore structure.

1 Introduction

Freshwater shortage resulted from elevated demand for water resources as well as the irrational exploitation and use after economic and population growth (Zhang and Xie 2019; Prajapati et al. 2021), constrains the sustainability of agricultural production (Aparicio et al., 2019). Alternative water resources with variable water quality (such as saline water) are being considered for agricultural irrigation in several desert and saline areas (Singh et al. 2021; Liu et al. 2022a). Utilizing saline water could partly alleviate the undersupply of freshwater for agricultural production (Yang et al., 2020). However, the other side of the coin is that saline water irrigation could result in soil salinization and/or sodicity. Once the soil is salinized and/or alkalized, soil hydraulic properties, like infiltration rate, saturated hydraulic conductivity and permeability, will change inevitably (Scudiero et al., 2017). And cations in the soil solution change the soil structural characteristics through the soil clay particle dispersion and flocculation (Bouksila et al. 2013; Hack-ten Broeke et al. 2016; Zhang et al. 2018). Therefore, in order to optimize saline water utilization, the effects of saline water quality on the soil

hydraulic properties and pore structure characteristics should be paid more attention.

Saline water irrigation can increase the monovalent ions concentration in soil solution and affect soil structure (Qadir et al. 2007; Qadir et al. 2021). Excess sodium (Na^+) from saline irrigation water is adsorbed onto the clay surface in salt-affected soils where sodium compounds predominate contributing to the disintegration of soil structure (Marchuk and Rengasamy 2011; Belkheiri and Mulas 2013; Awedat et al. 2021). As percolation progresses, the thickness of the diffusion double electron layers increases due to the relatively larger hydrated radius of Na^+, and the repulsive force between adjacent diffusion double electron layers appears to increase, resulting in the dispersion and swelling of soil particles (Alva et al. 1991; Reading et al. 2015).

Soil calcium (Ca^{2+}) and magnesium (Mg^{2+}) can alleviate soil dispersibility by replacing Na^+ in soil colloids, the outer layers of the Ca^{2+} and Mg^{2+} containing colloidal particles do not adsorb water molecules, turning Na^+ qualitative hydrophilic colloid into Ca^{2+} and Mg^{2+} hydrophobic colloids (Marchuk and Rengasamy 2011; Tsai et al. 2012). Colloidal particles move closer to each other, promoting soil particles forming water stable aggregates, thus improving soil structural stability (Gharaibeh et al. 2009; McKenna et al. 2019). Therefore, the concentration of Na^+ in relation to Mg^{2+} and Ca^{2+} (sodium adsorption ratio, SAR) (U.S. Salinity Laboratory Staff 1954) is a crucial criterion for soil structural stability and hydraulic conductivity (Rengasamy and Marchuk 2011). Although SAR can be used to predict soil clay dispersion effect caused by cations, the controlling mechanism of dispersion in SAR is presumed to be

exchangeable Na^+. However, Na^+ does not alone cause soil dispersion since the chemical component of clay structure integrity is mainly a function of ionic valence and hydration radius (Marchuk et al., 2014). Potassium (K^+) has been overlooked because salt-affected soils typically contain low amounts of K^+. However, Li et al. (2022) reported that under the continuous recycling use of underground saline water, water-soluble and exchangeable K^+ is higher than Ca^{2+} and Mg^{2+} in the Hetao irrigation district—one of the large irrigation districts in China. It is anticipated that the long-term use of irrigation water with high K^+ concentrations may therefore create substantial challenges in preserving good soil structure and adequate infiltration rates (Sposito et al., 2016). K^+ is not as effective as Na^+ in generating soil particle dispersion and swelling problems, yet Marchuk and Marchuk (2018) pointed out that K^+ could substitute Na^+ on exchange sites to encourage Na^+ leaching and increase water conductivity to some extent. A lower concentration of K^+ may have positive effects on soil permeability due to the substitution of exchangeable Na^+ by K^+ with lower dispersive potential, increasing aggregates stability and soil pore connectivity (Buelow et al., 2015). Traditional SAR ignored the role of K^+, a newly proposed equation, cation ratio of soil structural stability (CROSS) could integrate the effects of Na^+ and K^+ in soil, which is an important indicator for assessing the quality of saline water (Rengasamy and Marchuk 2011).

Thus, we hypothesized that the amount of K^+ relative to Na^+ would certainly have an effect on soil structural stability, which could be evaluated in a column experiment

under controlled conditions. The specific objectives of this study were to (1) ascertain the effect of irrigation saline water with different relative concentrations of K^+ to Na^+ (K^+/Na^+) on transport and distribution of water and salt; (2) determine the effect on soil pore structural characteristics; (3) predict these effects using a newly proposed index (CROSS) rather than SAR.

2 Materials and methods

2.1 Soil sampling location and properties

The study soil was collected from a layer of 0–40 cm field in Yangling (108°04′E, 34°20′N), Shaanxi Province, China. After air-dried, the soil was grounded to pass through a 2-mm seize. Soil's physical and chemical properties are listed in Table 1. Soil particle size distribution was measured by the Laser Mastersizer 2000 (Malvern Instruments, Malvern, UK), and according to the international classification system, soil texture was classified as silty clay. Soil bulk density was calculated usnig the soil core method. EC_e and pH were measured using conductivity meter (DDS-307, China) and pH meter (PHS-3C, China), respectively. Total soluble salts refer to the total amount of soluble salts in soil-saturated paste extract. Flame photometry (6400A, China) was used to measure soluble Na^+ and K^+, concentrations of CO_3^{2-} and HCO_3^- were tested using the neutral titration method, Cl^- was analyzed using the silver nitrate titration method, and SO_4^{2-} was determined using barium sulfate turbidimetric method, Mg^{2+} and Ca^{2+} were specified using ethylene diamine tetraacetic acid (EDTA)

121 titrimetric method (Bao 2005).

122 Table 1 The physicochemical properties of study soil.

Property	Value
Particle size distribution (%)	
Sand (> 0.05 mm)	8.10
Silt (0.05–0.002 mm)	60.62
Clay (< 0.002 mm)	31.28
Texture	Silty clay
EC_e (dS m^{-1})	0.72
pH	7.66
Total soluble salts (g Kg^{-1})	0.14
Ion concentration (mmol L^{-1})	
CO_3^{2-}+HCO_3^-	0.60
Cl^-	0.23
SO_4^{2-}	2.18
Mg^{2+}	0.32
Ca^{2+}	0.54
Na^+	0.10
K^+	< 0.01

123 Note: EC_e is electrical conductivity of soil-saturated extract.

124 **2.2 Experimental design**

125 Soil columns were prepared using transparent polyvinyl chloride cylinders, with
126 an internal diameter of 20 cm and a height of 50 cm (Fig. 1). Round and small holes (6
127 mm diameter) were arranged equally at the bottom of each cylinder for drainage. A 5
128 cm depth quartz sand was laid at the bottom of the soil column as a filter layer before
129 packing to prevent small soil particles from being washed away. After that, air-dried
130 soil was packed at 40 cm height with a bulk density of 1.35 g cm^{-3} (referring to the
131 original level of the soil). The sieved dry soil was poured into each soil column in the

5-cm sections for uniform compaction, and the layer's surface was roughened to ensure a tight connection to the next layer. The soil column was then allowed to stand in the laboratory for 24 hours before starting the experiments described herein. The constant water head (2 cm, using a Mariotte bottle) infiltration experiment was conducted with 3 replications for each treatment.

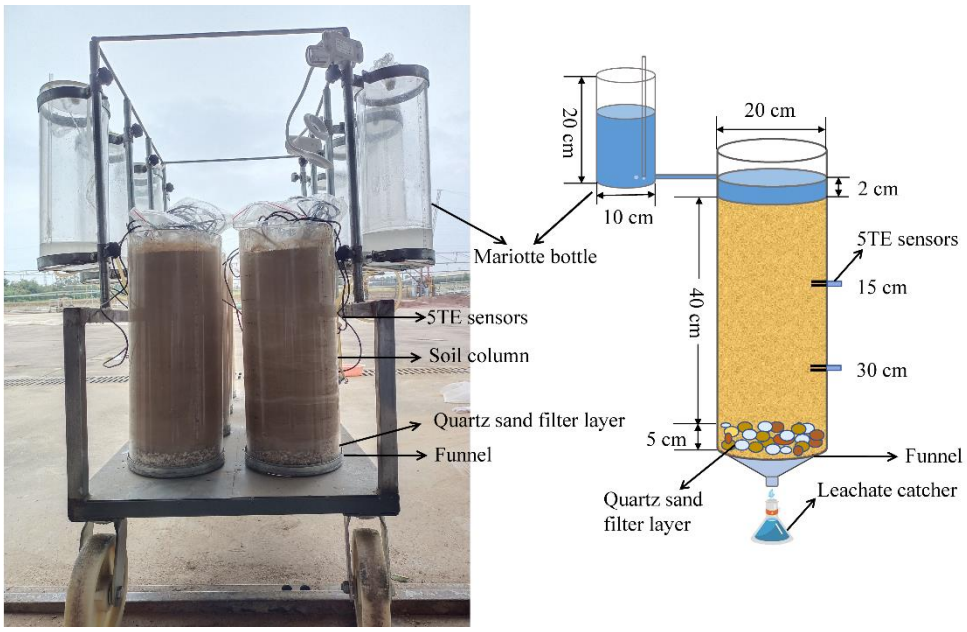

Fig. 1. Illustration of the experiment apparatus (a) and schematic diagram (b).

Three infiltration solutions were prepared with different ratios of K^+/Na^+ [(0:1 (K0Na1), 1:1 (K1Na1), 1:0 (K1Na0)] at constant EC of 4 dS m^{-1}, with deionized water was used as the control (CK) (Table 2). The cation ratio of soil structural stability (CROSS) (Rengasamy and Marchuk 2011) is an indicator of soil structural behavior as influenced by both Na^+ and K^+, and it was calculated as follows (Smith et al., 2015):

$$CROSS = \frac{Na^+ + 0.335K^+}{\left[\left(Ca^{2+} + 0.0758Mg^{2+}\right)/2\right]^{0.5}} \quad (1)$$

where the chemical element symbols denote charge concentrations ($mmol_c$ L^{-1}).

146 Table 2 Saline water settings with different K^+/Na^+ at a constant EC.

Treatment	Added salt/ (mmol L^{-1})			K^+/Na^+	Setting EC (dS m^{-1})	Measured EC (dS m^{-1})	CROSS ($mmol_c$ $L^{-1})^{0.5}$
	KCl	NaCl	$CaCl_2$				
K0Na1	0	34	3	0:1	4.00	4.25	27.76
K1Na1	17	17	3	1:1	4.00	4.33	17.49
K1Na0	34	0	3	1:0	4.00	4.40	7.22
CK	Deionized water			/	0.00	0.02	/

147 Note: K0Na1, K1Na1 and K1Na0 indicate the saline water at EC of 4 dS m^{-1} with
148 K^+/Na^+ of 0:1, 1:1 and 1:0, respectively; CK, deionized water; CROSS represents cation
149 ratio of soil structural stability.

150 The experiment implemented alternate leaching, as the prolonged leaching process
151 of soil substrates is more helpful in illuminating the function of electrolyte effect and
152 cation exchange (Shaygan et al., 2017). The next infiltration was performed two days
153 after the drainage of the previous infiltration was completed. Soil layers were regarded
154 as reaching desalination prerequisite when the soil salt content came to less than 0.3%,
155 which meant that bulk electrical conductivity was less than 1.5 dS m^{-1} (transformation
156 from salt content to bulk electrical conductivity) (Yin et al., 2022). Water application
157 was stopped when the bulk electrical conductivity of all treatments at 15 cm depth
158 reached the prerequisite for desalination. This experiment was planned to fill all the
159 pores in the soil column throughout the infiltration cycle, therefore the water applied at
160 the first infiltration was described by the pore volume equation (Xu and Huang 2010):

161 $$V_p = V_s \cdot TP \quad (2)$$

162 $$TP = \frac{ds - BD}{ds} \quad (3)$$

163 where V_p is the pore volume (cm^3), V_s is the volume of filled soil (cm^3), TP is the soil

164 total porosity (%), *ds* is the soil particle density (2.65 g cm^{-3}) (Xu and Huang 2010),
165 *BD* is the bulk density (g cm^{-3}). According to Eq. (2) and Eq. (3), around 6 L of water
166 was required in the first infiltration. Required water volume for each subsequent
167 leaching was determined by the volume of leachate at the first infiltration, 0.5 L each
168 time.

169 **2.3 Soil properties measurements**

170 During the whole experimental period, soil volumetric water content and bulk
171 electrical conductivity were real-time monitored at 15 and 30 cm soil depths from the
172 soil surface by capacitance sensors (ECH2O 5TE, METER Group, USA) (Fig. 1).
173 Leachate was collected in the leachate catcher below the soil column. Cumulative
174 leachate volume was monitored over time to determine the saturated hydraulic
175 conductivity (K_{sat}, cm min^{-1}) of each treatment by using a derivation of Darcy's
176 approach (Sahin et al., 2011):

177 $$K_{sat} = \frac{V_l \cdot H}{A \cdot t \cdot (H + h)} \quad (4)$$

178 where V_l is the leachate volume (cm^3), *H* is the length of filled soil (cm), *A* is the surface
179 area of soil column (cm^2), *t* is the leaching time of measurement (min), *h* is the height
180 of constant water head (cm).

181 To determine the amount of salt released, we measured the volume and EC of the
182 leachate. The leachate was collected at 3 h intervals when the leachate started to drain,
183 and leachate was stored in 100 ml wide-mouth polypropylene reagent bottles. The salt

accumulated in the soil column was determined by subtracting the salt in the leachate from the applied water, the salination rate (*Rs*, %) indicated the ratio of salt accumulated in the soil column at every time of infiltration to the salt content at the first applied water. Leaching efficiency (*Le*, g L^{-1}) refers to the amount of desalination per unit of water volume in the desalination process. *Rs* and *Le* were calculated as follows:

$$Rs = m_s / m_w \quad (5)$$

$$Le = (m_s - m_1) / w \quad (6)$$

Where m_s is the salt content accumulated in soil column at each infiltration (g), m_w is the salt content in the total water used for the first infiltration (g), m_1 is the mass of salts after the first infiltration (g), w is the total water volume used for leaching (L).

Soil samples were collected from each soil column at 5-cm intervals with the 0–40 cm soil layer three days after the final infiltration. Soil *BD* was calculated using the soil core method, and *TP* was calculated by Eq. (3) based on *BD*. Soil water characteristics curve was measured with the high velocity centrifugal method (CR21 Hitachi, Japan), and calibrated by RETC software (PC Progress Inc., Prague, Czech Republic). Currently, several defining sizes of macropores are proposed, rather than a precise definition and pore size range (Cameira et al. 2003; Kim et al. 2010; Hu et al. 2018; Budhathoki et al. 2022; Aldaz-Lusarreta et al. 2022). In this study, macropores were defined as the pores with diameters larger than 1 mm, whereas micropores were defined as smaller than 1 mm (Luxmoore 1981; Wilson and Luxmoore 1988). Based on the capillary pressure data, the relationship between pore diameter (*d*, mm) and water

205 suction (S, Pa) was described according to the capillary bundle model (Jury et al., 1991):

206 $$d = \frac{300}{S} \quad (7)$$

207 **2.4 Statistical analysis**

208 Statistical analysis among all treatments with different K^+/Na^+ was performed in
209 SPSS 22.0 software, using one-way analysis of variance (ANOVA) based on the least
210 significant difference (LSD) test at 95% significance level ($P < 0.05$). All figures were
211 created through Origin 2022b.

212 **3 Results**

213 **3.1 Soil saturated hydraulic conductivity (K_{sat})**

214 The K0Na1, K1Na1 and K1Na0 significantly ($P < 0.05$) reduced K_{sat} by 43.62%,
215 29.04% and 18.06% compared with CK, respectively (Fig. 2). Additionally, K_{sat} was
216 negatively correlated with CROSS of saline water, increasing the CROSS of the applied
217 saline water generally reduced K_{sat}.

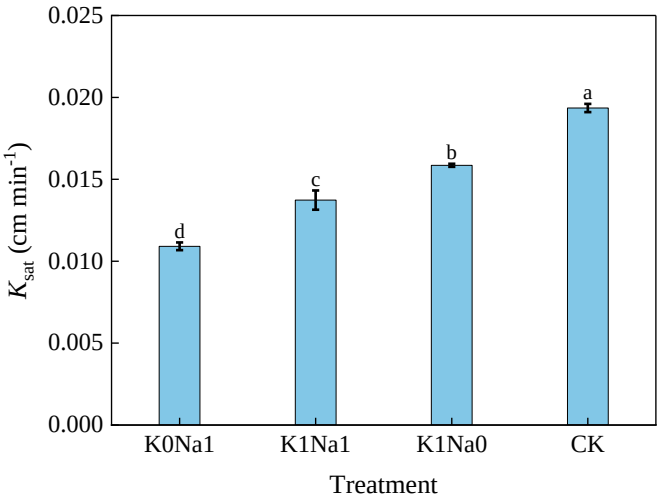

Fig. 2. Saturated hydraulic conductivity (K_{sat}) under different treatments. K0Na1, K1Na1 and K1Na0 indicate the saline water at EC of 4 dS m^{-1} with K^+/Na^+ of 0:1, 1:1 and 1:0, respectively; CK, deionized water; Different letters after means of K_{sat} indicate statistical differences ($P < 0.05$) among treatments based on LSD. Bars indicate standard deviations of means.

3.2 Soil water content

Water content increased immediately after each infiltration in all treatments, then gradually decreases and the degree of variation tends to stabilize (Fig. 3). And water content at deeper soil depths was greater than at shallow soil depths at the same time during the whole infiltration period. The water content ranged from 0.39–0.41 and 0.40–0.42 cm^3 cm^{-3} at 15 and 30 cm soil depths, respectively. K0Na1 had the highest water content at both 15 and 30 cm soil depths. K1Na1 and K1Na0 were greater than CK at 15 cm soil depth and lower than CK at 30 cm soil depth, and the water content of K1Na1 was higher than K1Na0 at both 15 and 30 cm soil layers.

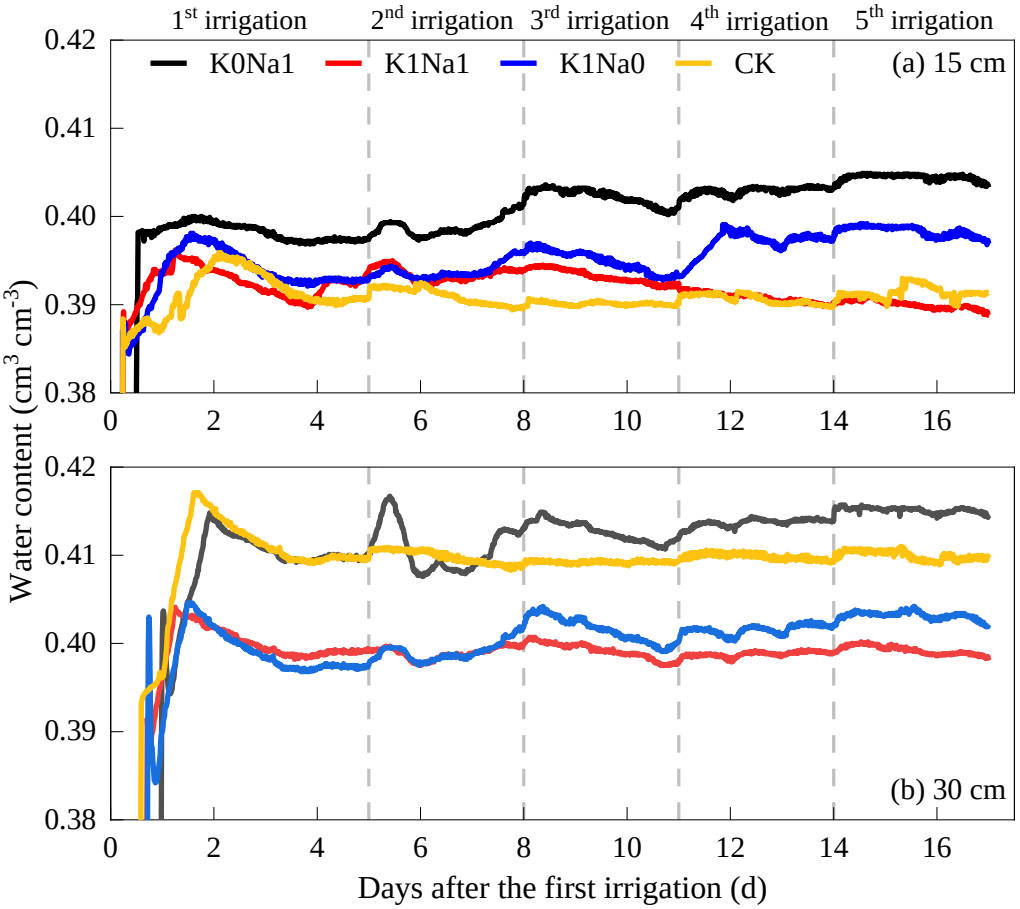

Fig. 3. Variation of water content over time under different treatments at 15 (a) and 30 cm (b) soil depths during the five times of infiltration.

3.3 Soil salination rate (*Rs*) and leaching efficiency (*Le*)

The *Rs* and *Le* under CK were not shown in Fig. 4, because deionized water was used as the control and there was almost no salt contained in the study soil, CK was considered negligible for salt accumulation and leaching. *Rs* peaked at the first infiltration, and approximately 70%–80% of the salt in the saline water was retained in the soil column, after which the subsequent leaching had lower *Rs* values (Fig. 4). The lower the relative concentration of K^+ to Na^+, the larger soil *Rs*. Among the three saline

243 water treatments, K1Na0 had the lowest *Rs* and highest *Le* at five infiltrations.

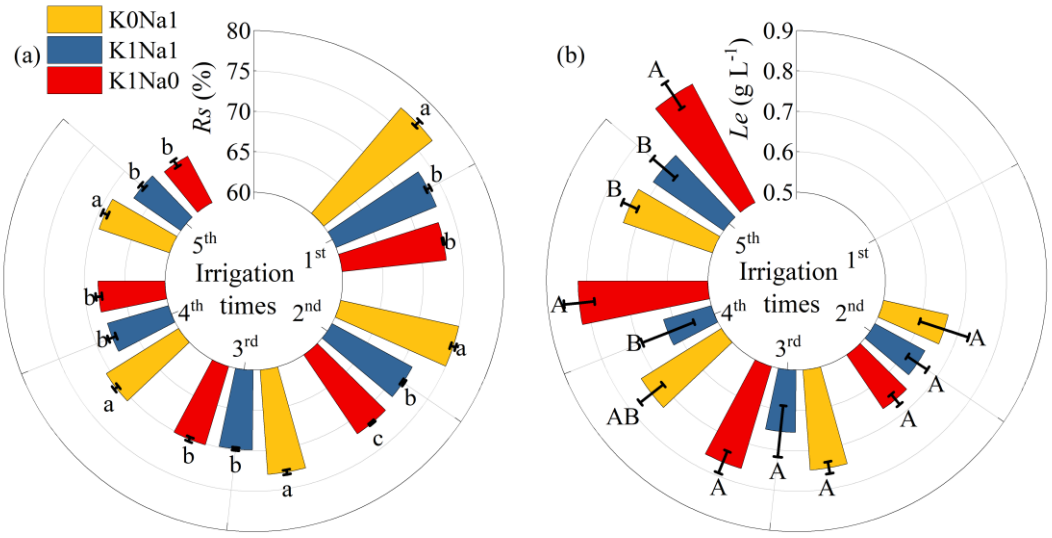

244

245 Fig. 4. Salination rate (*Rs*) (a) and leaching efficiency (*Le*) (b) at five infiltrations under
246 all saline water treatments. K0Na1, K1Na1 and K1Na0 indicate the saline water at EC
247 of 4 dS m^{-1} with K^+/Na^+ of 0:1, 1:1 and 1:0, respectively; Different lowercase letters
248 followed means of *Rs* indicate statistical differences ($P < 0.05$) among treatments based
249 on LSD, and different uppercase letters followed means of *Le* indicate statistical
250 differences ($P < 0.05$) among treatments based on LSD. Bars indicate standard
251 deviations of means.

252 **3.4 Soil bulk electrical conductivity**

253 Bulk electrical conductivity of K0Na1, K1Na1 and K1Na0 ranged from 1.0–2.0
254 dS m^{-1} at 15 cm, 1.5–2.5 dS m^{-1} at 30 cm soil depth (Fig. 5). After the first infiltration,
255 bulk electrical conductivity in 15 cm soil depth peaked, and then exhibited a general
256 downward trend in the following infiltrations. However, more salts were leached to

deeper layers, where salt began to accumulate instead of desalination, and bulk electrical conductivity at 30 cm soil depth gradually increased following the infiltration events. Overall, K0Na1 had the highest bulk electrical conductivity among all treatments at both 15 and 30 cm, and K1Na1 was quite higher than K1Na0.

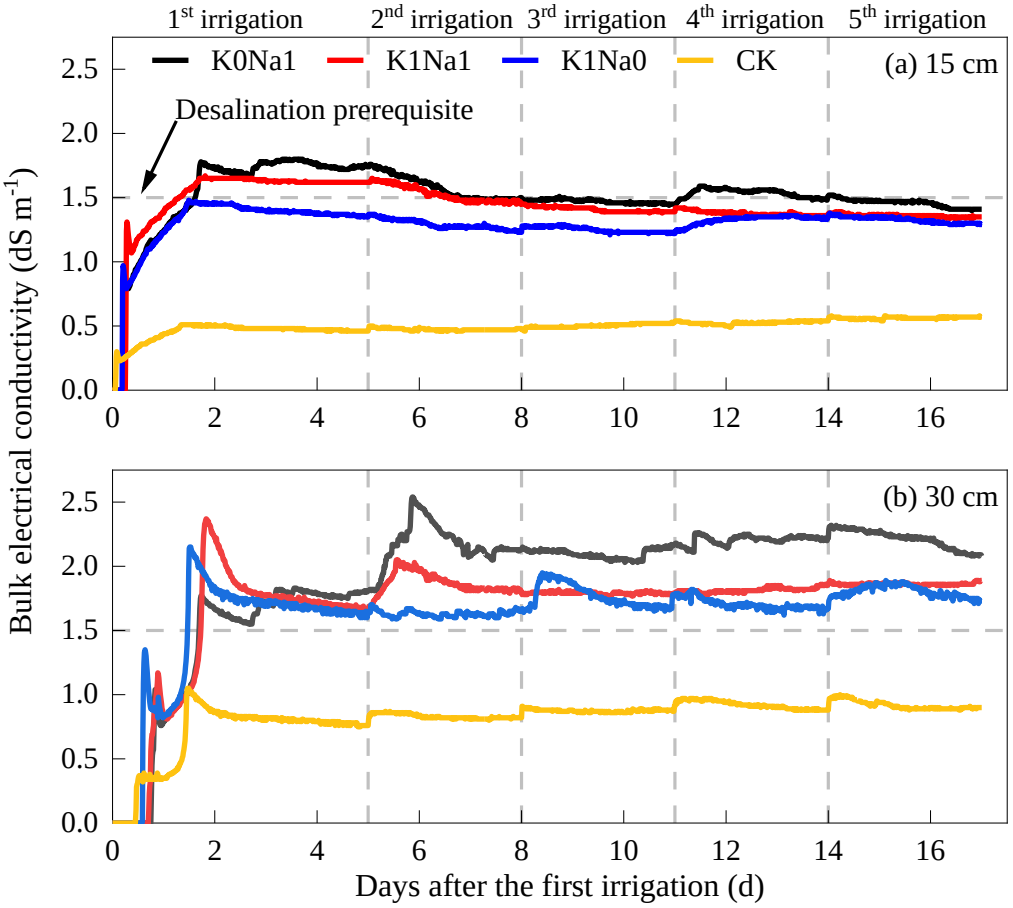

Fig. 5. Variation of bulk electrical conductivity over time under treatments with different K^+/Na^+ at constant EC at 15 (a) and 30 cm (b) soil depths in the period of five times of infiltration. K0Na1, K1Na1 and K1Na0 indicate the saline water at EC of 4 dS m^{-1} with K^+/Na^+ of 0:1, 1:1 and 1:0, respectively; CK, deionized water.

At 15 cm soil depth, K0Na1 reached the soil desalination prerequisite after the fifth infiltration, while K1Na1 reached the desalination prerequisite after the second infiltration, and K1Na0 did not exceed desalination prerequisite during the whole

infiltration period. Among all saline water treatments, K1Na0 reduced the desalination time and required leaching volume to reach the standard of desalination. K0Na1, K1Na1 and K1Na0 did not meet the desalination prerequisite at 30 cm soil depth, and the increased volume of infiltration water also increased the bulk electrical conductivity.

3.5 Soil bulk density (*BD*) and total porosity (*TP*)

Soil *BD* varied from 1.30–1.40 g cm^{-3} across all treatments, and *BD* was below 1.35 g cm^{-3} at 0–10 and 35–40 cm soil layers, however, over 1.35 g cm^{-3} at 10–35 cm soil depth (Fig. 6). K0Na1 significantly ($P < 0.05$) enhanced soil *BD* throughout the soil column profile compared with CK. *TP* first diminished with soil depth to reach a minimum at about 30–35 cm, and then slightly increased at 35–40 cm. The *TP* of K1Na1 and K1Na0 slightly improved after five times of infiltration, and only K0Na1 showed a decline compared with CK. Overall, over the whole infiltration period, K1Na0 was most conducive to the formation of soil pore structure and increasing the total pore volume. The saline water with lower CROSS was beneficial for reducing soil *BD* and increasing *TP*.

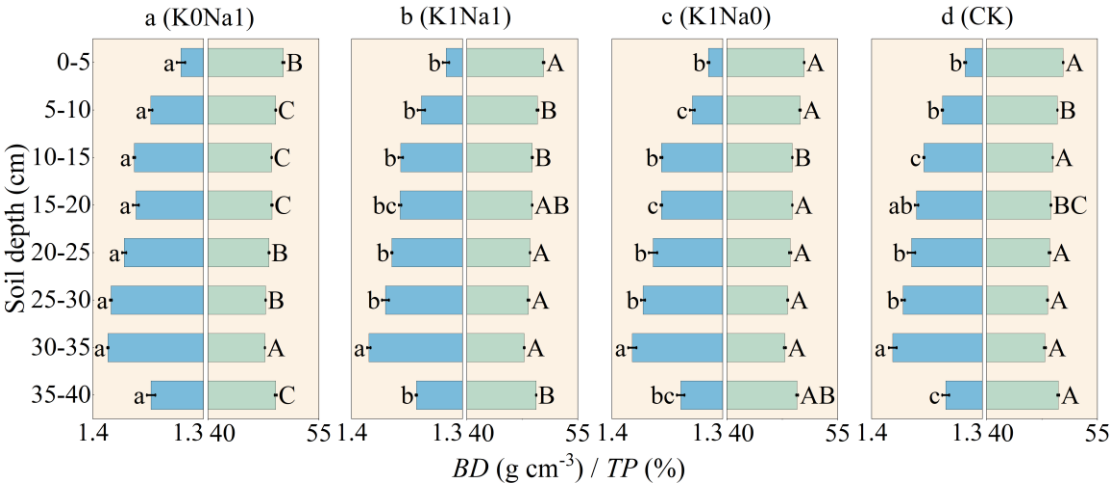

Fig. 6. Soil bulk density (*BD*) and total porosity (*TP*) throughout the soil column profile under different treatments. K0Na1, K1Na1 and K1Na0 indicate the saline water at EC of 4 dS m^{-1} with K^+/Na^+ of 0:1, 1:1 and 1:0, respectively; CK, deionized water; The blue horizon columns represent *BD*, while the green horizon columns represent *TP*; Different lowercase letters followed means of *BD* indicate statistical differences ($P < 0.05$) among treatments based on LSD, and different uppercase letters followed means of *TP* indicate statistical differences ($P < 0.05$) among treatments based on LSD. Bars indicate standard deviations of means.

3.6 Proportion of micropores and proportion of macropores

Micropores were the dominant pores for all treatments, the proportion of micropores accounting for more than 40% of the total soil volume, however, the proportion of macropores did not exceed 8% (Fig. 7). The 0–5 cm soil layer had the lowest proportion of macropores and retained the largest proportion of micropores compared with other depths. K0Na1 had the highest proportion of micropores and the

299 lowest proportion of macropores. K1Na0 had a greater proportion of macropores in the

300 soil column than CK.

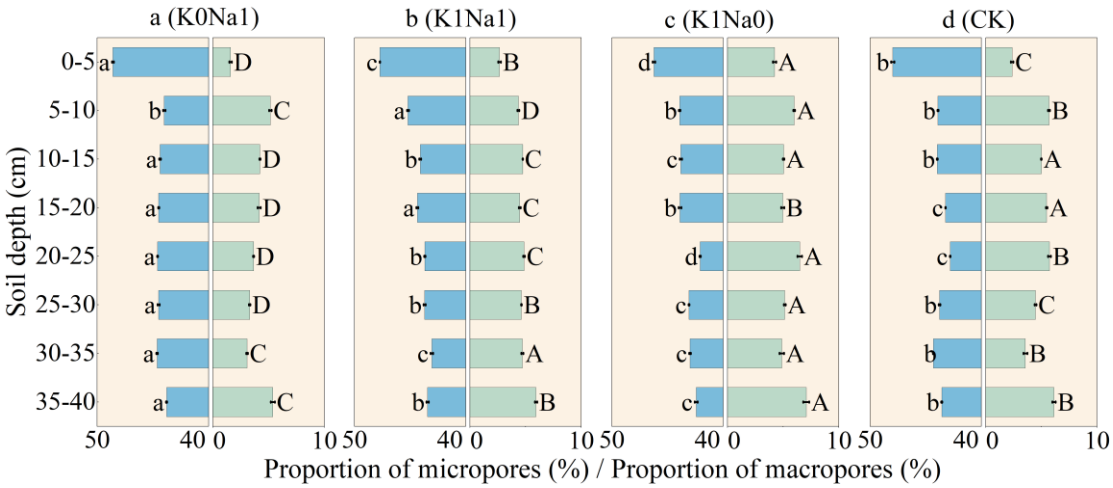

301

302 Fig. 7. Proportion of micropores and proportion of macropores in total soil volume

303 throughout the soil column profile under different treatments. K0Na1, K1Na1 and

304 K1Na0 indicate the saline water at EC of 4 dS m^{-1} with K^+/Na^+ of 0:1, 1:1 and 1:0,

305 respectively; CK, deionized water; The blue horizon columns represent proportion of

306 micropores, while the green horizon columns represent proportion of macropores;

307 Different lowercase letters followed means of proportion of micropores indicate

308 statistical differences ($P < 0.05$) among treatments based on LSD, and different

309 uppercase letters followed means of proportion of macropores indicate statistical

310 differences ($P < 0.05$) among treatments based on LSD. Bars indicate standard

311 deviations of means.

4 Discussion

4.1 Effects of saline water on soil water movement and redistribution

As a crucial soil hydraulic characteristic, K_{sat} reflects the transportation ability of water and solutes (Braud et al. 2001; Maillard et al. 2011; Albalasmeh et al. 2022). The cation composition and EC of soil solution affect K_{sat} by controlling electrostatic repulsive pressure through surface potential and midpoint potential between adjacent particles, and consequently influence water movement (Fares et al. 2000; Liu et al., 2022b). Specifically, the relative concentration of K^+ to Na^+ in saline water was related to the swelling and dispersion of soil particles (Yu et al. 2016; Zhu et al. 2019). Dispersed clay particles clogged soil macropores to subsequently restrict water transport (Awedat et al., 2021). The Na^+ has a relatively higher ionicity index than K^+, as a result, the low relative concentration of K^+ to Na^+ decreased the degree of covalency in clay-cation bonds, which was detrimental to clay particles aggregation (Marchuk and Rengasamy 2011). Therefore, in our study, the high relative concentration of K^+ to Na^+ promoted the flocculation and stabilization of soil clay particles, resulting in an increased water hydraulic conductivity (Fig. 2).

After a certain period of irrigation, soil moisture redistributed at different depths of soil column (Fig. 3). Soil water moved further down during the phase of water redistribution soon after each irrigation, reducing the water content in the upper soil layers. As the upper soil layers drained, the lower soil layers still had water inflow

(Kargas et al., 2021), increasing the water content in the lower soil layers. The results also implicated that the retention of soil water by Na^+ was stronger than that by K^+, the cause may be that Na^+ can increase the thickness of the diffuse-double layers around soil colloids theoretically due to its larger hydrated radius and lower charge than K^+, and the adjacent double layers overlapped to provide more space between layers (He et al., 2015), where, subsequently, more water can be retained (Fig. 3).

Additionally, our study showed that K1Na1 was even more beneficial than deionized water for water downward transport (Fig. 3), which was due to that deionized water (CK) (below 0.2 dS m^{-1}) tended to leach soluble minerals and salts, especially Ca^{2+}, from the surface soil layers. This would lead to the reduction of its original solid soil structural stability. In the absence of salt and Ca^{2+}, the dispersed tiny particles filled the smaller pore spaces in soil, reducing even more channels for water flow and exacerbating water retention in deeper soil layers (Ayers and Westcot 1985). However, a lower concentration of soluble salts could increase colloid flocculation, and thereby, improving soil aeration and water conductivity (Tang and She 2016).

4.2 Effects of saline water on soil salination and desalination process

Numerous factors influence soil salt leaching efficiency; for example, increasing EC and reducing SAR definitely improve clay flocculation, which can enhance salt leaching (Ebrahim Yahya et al., 2022). Na^+ is more likely to trigger soil clay dispersion and swelling than K^+, thus Na^+ generally inhibits water infiltration, which is detrimental

352 to salt leaching (Smiles and Smith 2004). Adding K^+ could promote displacement of
353 the adsorbed Na^+, and then decrease Na^+ concentration and salt accumulation in soil
354 solute through leaching.

355 A greater reduction in Na^+ concentration was associated with a higher rate of
356 cation exchange rate, and the slow rate of solute leaching from aggregates reduced the
357 total leaching efficiency (Shaygan et al., 2017). During the leaching process, water flow
358 preferentially passed through the macropores rather than aggregates. The slow water
359 transportation through aggregates induced the slow removal of solutes from the
360 aggregates, leading to a reduced leaching efficiency. In our study, the alternate leaching
361 was implemented to improve solute leaching (Figs. 4 and 5). The soil solutes diffused
362 into the aggregates surface during the rest period, improving salt leaching due to the
363 water flow in macropores (Al-Sibai et al., 1997). Saline water with more K^+ could
364 increase the magnitude of cation exchange due to the substitution of Na^+ on exchange
365 sites by K^+ with lower dispersive potential (Shaygan et al., 2017), the intensive release
366 of cations from the soil further improved salt's leaching efficiency. In addition, the
367 integrity of soil aggregates created by combining clay particles and the other soil
368 components enhanced by K^+ can benefit solute transportation (Marchuk and
369 Rengasamy 2011).

370 **4.3 Effects of saline water on soil pore structure characteristics**

371 The upper soil was longer exposed to water due to the long-term continuous

372 irrigation, causing the particles to swell and the surface layer to loosen (Vaezi et al.
373 2017; Håkansson and Lipiec 2000), and also the decreased *BD* in the surface layer of
374 soil column (Fig. 6). The subsoil *BD* increased with depth under the impact of water
375 pressure and self-weight due to the declining pore diameter and pore branching closure
376 (Schjønning et al., 2013). And for soil at the bottom, the loss of soil particles from small
377 holes was responsible for the abrupt reduction in *BD* (Fig. 6). The value of CROSS in
378 saline water could reflect changes in soil *BD* and *TP*, in agreement with the result of
379 Marchuk and Marchuk (2018). The high CROSS implied an increase in the proportion
380 of monovalent exchangeable cations, thickening the double layer at the interface
381 between the clay surface and soil solution. Hence, soil swelling occurred at the expense
382 of water-conducting pores. Additionally, aggregates slaking and subsequent clay
383 dispersion and deposition of clay particles within the pore space contributed to the
384 reduction in *TP* (Marchuk and Marchuk 2018).

385 Soil macropores play a crucial role in water and solute transport, accounting for
386 85% of the total infiltration volume (Wilson and Luxmoore 1988; Weiler and Naef 2003;
387 Kotlar et al. 2020). For saline water with the same EC, a decrease in K^+ concentration
388 may enhance soil clay dispersion, resulting in the loosening of clay particles from the
389 aggregates. This, in turn, dispersed clay particles moved with water caused the
390 macropores to become blocked, converting them into micropores (Cameira et al., 2003),
391 thus leading to a decrease in the volume of soil macropores (Fig. 7).

5 Conclusion

We explored the effects of the relative ratio of K^+ to Na^+ in saline water on soil hydraulic characteristics and structural stability via a soil column experiment. Irrigation with saline water of K^+/Na^+ of 1:0 caused fewer pore blockages due to soil clay particle dispersion than 0:1, which increased soil saturated hydraulic conductivity. The presence of K^+ accelerated the sustained Na^+ replacement and leaching, alleviating salt accumulation and enhancing leaching efficiency. K^+ positively affected the establishment of soil structure due to the transformation of micropores into macropores, and the ever-increasing unobstructed water-conducting channels sped up water and solute transport. The rational use of saline water with adequate K^+ could help mitigate the structural deterioration caused by Na^+. Appropriate adjustment of the relative concentration of K^+ to Na^+ in saline water during infiltration could ameliorate soil structural properties. In addition to Ca^{2+} and Mg^{2+} (primary concerns in earlier studies), the relative concentration of K^+ to Na^+ is an essential indicator for assessing the suitability of saline water quality for irrigation and should be considered when using saline water.

Author contributions

Sihui Yan and Tibin Zhang conceived and designed the experiments. Sihui Yan, Binbin Zhang and Tonggang Zhang led the data processing and statistical analysis, Sihui Yan, Yu Cheng, Chun Wang and Min Luo performed the experiments. Sihui Yan

wrote the initial draft. Hao Feng and Kadambot H.M. Siddique contributed to review and editing of the paper.

Acknowledgments

This work was supported by the National Key R&D Program of China (Grant No. 2021YFD1900700), the Innovation Capability Support Program of Shaanxi (Grant no. 2022PT-23), the Key R&D Program of Shaan xi (Grant no. 2023-ZDLNY-53), and China 111 project (B12007).

References

Albalasmeh, A., Mohawesh, O., Gharaibeh, M., Deb, S., Slaughter, L., El Hanandeh, A.: Artificial neural network optimization to predict saturated hydraulic conductivity in arid and semi-arid regions, Catena, 217, 106459, http://dx.doi.org/10.1016/J.CATENA.2022.106459, 2022.

Aldaz-Lusarreta, A., Giménez, R., Campo-Bescós, M.A., Arregui, L.M., Virto, I.: Effects of innovative long-term soil and crop management on topsoil properties of a Mediterranean soil based on detailed water retention curves, SOIL, 8, 655-671, http://dx.doi.org/10.5194/SOIL-8-655-2022, 2022.

Al-Sibai, M., Adey, M.A., Rose, D.A.: Movement of solute through a porous medium under intermittent leaching, Eur. J. Soil Sci., 48, 711-725, http://dx.doi.org/10.1046/j.1365-2389.1997.00126.x, 1997.

Alva, A.K., Sumner, M.E., Miller, W.P.: Relationship between ionic strength and electrical conductivity for soil solutions, Soil Sci., 152, 239-242, https://doi.org/10.1097/00010694-199110000-00001, 1991.

Aparicio, J., Tenza-Abril, A.J., Borg, M., Galea, J., Candela, L.: Agricultural irrigation of vine crops from desalinated and brackish groundwater under an economic perspective. A case study in Siġġiewi, Malta, Sci. Total Environ., 650, 734-740, https://doi.org/10.1016/j.scitotenv.2018.09.059, 2019.

Awedat, A.M., Zhu, Y., Bennett, J.M., Raine, S.R.: The impact of clay dispersion and migration on soil hydraulic conductivity and pore networks, Geoderma, 404, 115297, http://dx.doi.org/10.1016/J.GEODERMA.2021.115297, 2021.

Ayers, R.S., Westcot, D.W.: Water Quality for Agriculture, FAO Irrigation and Drainage Paper 29 Rev 1, Rome, Italy.

Bao, S.D.: Soil Analysis in Agricultural Chemistry, China Agricultural Press,Beijing, China, 2005 (in Chinese).

Belkheiri, O., Mulas, M.: The effects of salt stress on growth, water relations and ion accumulation in two halophyte Atriplex species, Environ. Exp. Bot., 86, 17-28, http://dx.doi.org/10.1016/j.envexpbot.2011.07.001, 2013.

Bouksila, F., Bahri, A., Berndtsson, R., Persson, M., Rozema, J., Van der Zee, S.E.A.T.M.: Assessment of soil salinization risks under irrigation with brackish water in semiarid Tunisia, Environ. Exp. Bot., 92, 176-185, http://dx.doi.org/10.1016/j.envexpbot.2012.06.002, 2013.

Braud, I., Vich, A.I.J., Zuluaga, J., Fornero, L., Pedrani, A.: Vegetation influence on runoff and sediment yield in the Andes region: observation and modelling, J. Hydrol., 254, 124-144, http://dx.doi.org/10.1016/S0022-1694(01)00500-5, 2001.

Budhathoki, S., Lamba, J., Srivastava, P., Malhotra, K., Way, T.R., Katuwal, S.: Using X-ray computed tomography to quantify variability in soil macropore characteristics in pastures, Soil Tillage Res., 215, 105194, http://dx.doi.org/10.1016/J.STILL.2021.105194, 2022.

Buelow, M.C., Steenwerth, K., Parikh, S.J.: The effect of mineral-ion interactions on soil hydraulic conductivity, Agric. Water. Manag., 152, 277-285, http://dx.doi.org/10.1016/j.agwat.2015.01.015, 2015.

Cameira, M.R., Fernando, R.M., Pereira, L.S.: Soil macropore dynamics affected by tillage and irrigation for a silty loam alluvial soil in southern Portugal, Soil Tillage Res., 70, 131-140,

http://dx.doi.org/10.1016/S0167-1987(02)00154-X, 2003.

Ebrahim Yahya, K., Jia, Z., Luo, W., Yuanchun, H., Ame, M.A.: Enhancing salt leaching efficiency of saline-sodic coastal soil by rice straw and gypsum amendments in Jiangsu coastal area, Ain Shams Eng. J., 13, 101721, http://dx.doi.org/10.1016/J.ASEJ.2022.101721, 2022.

Fares, A., Alva, A.K., Nkedi-Kizza, P., Elrashidi, M.A.: Estimation of soil hydraulic properties of a sandy soil using capacitance probes and Guelph Permeameter, Soil Sci. Soc. Am. J., 165, 768-777, https://doi.org/10.1097/00010694-200010000-00002, 2000.

Gharaibeh, M.A., Eltaif, N.I., Shunnar, O.F.: Leaching and reclamation of calcareous saline-sodic soil by moderately saline and moderate-SAR water using gypsum and calcium chloride, J. Plant Nutr. Soil Sci., i.-Z. Pflanzenernahr. Bodenkd., 172, 713–719, http://dx.doi.org/10.1002/jpln.200700327, 2009.

Hack-Ten Broeke, M.J.D., Kroes, J.G., Bartholomeus, R.P., Van Dam, J.C., De Wit, A.J.W., Supit, I., Walvoort, D.J.J., Van Bakel, P.J.T., Ruijtenberg, R.: Quantification of the impact of hydrology on agricultural production as a result of too dry, too wet or too saline conditions, SOIL, 2, 391-402, http://dx.doi.org/10.5194/soil-2-391-2016, 2016.

Håkansson, I., Lipiec, J.: A review of the usefulness of relative bulk density values in studies of soil structure and compaction, Soil Tillage Res., 53, 71-85, http://dx.doi.org/10.1016/S0167-1987(99)00095-1, 2000.

He, Y.B., Desutter, T.M., Casey, F., Clay, D., Franzen, D., Steele, D.: Field capacity water as influenced by Na and EC: Implications for subsurface drainage, Geoderma, 245, 83-88, http://dx.doi.org/10.1016/j.geoderma.2015.01.020, 2015.

Hu, X., Li, Z.C., Li, X.Y., Wang, P., Zhao, Y.D., Liu, L.Y., LÜ, Y.L: Soil macropore structure characterized by X-Ray computed tomography under different land uses in the Qinghai Lake watershed, Qinghai-Tibet plateau., Pedosphere, 28, 478-487, http://dx.doi.org/10.1016/S1002-0160(17)60334-5, 2018.

Jury, W., Gardner, W.R., Gardner, W.H.: Soil Physics, John Wiley and Sons, New York, USA, 1991.

Kargas, G., Soulis, K.X., Kerkides, P.: Implications of hysteresis on the horizontal soil water redistribution after infiltration, Water, 13, 2773-2773, http://dx.doi.org/10.3390/W13192773, 2021.

Kim, H., Anderson, S.H., Motavalli, P.P., Gantzer, C.J.: Compaction effects on soil macropore geometry and related parameters for an arable field, Geoderma, 160, 244-251, http://dx.doi.org/10.1016/j.geoderma.2010.09.030, 2010.

Kotlar, A.M., de Jong van lier, Q., Andersen, H.E., Nørgaard, T., Iversen, B.V.: Quantification of macropore flow in Danish soils using near-saturated hydraulic properties, Geoderma, 375, 114479, http://dx.doi.org/10.1016/j.geoderma.2020.114479, 2020.

Li, Z.Y., Cao, W.G., Wang, Z.R., Li, J.C., Ren, Y.: Hydrochemical characterization and irrigation suitability analysis of shallow groundwater in Hetao Irrigation District, Inner Mongolia., Geoscience, 36, 418-426, https://doi.org/10.19657/j.geoscience.1000-8527.2022.012, 2022 (in Chinese).

Liu, B.X., Wang, S.Q., Liu, X.J., Sun, H.Y.: Evaluating soil water and salt transport in response to varied rainfall events and hydrological years under brackish water irrigation in the North China Plain, Geoderma, 422, 115954, http://dx.doi.org/10.1016/J.GEODERMA.2022.115954, 2022a.

503 Liu, X.M., Zhu, Y.C., Mclean Bennett, J., Wu, L.S., Li, H.: Effects of sodium adsorption ratio and
504 electrolyte concentration on soil saturated hydraulic conductivity, Geoderma, 414, 115772,
505 http://dx.doi.org/10.1016/J.GEODERMA.2022.115772, 2022b.
506 Luxmoore, R.J.: Micro-, meso-, and macroporosity of soils., Soil Sci. Soc. Am. J., 45, 671-672,
507 http://dx.doi.org/10.2136/sssaj1981.03615995004500030051x, 1981.
508 Maillard, E., Payraudeau, S., Faivre, E., Grégoire, C., Gangloff, S., Imfeld, G.: Removal of pesticide
509 mixtures in a stormwater wetland collecting runoff from a vineyard catchment, Sci. Total
510 Environ., 409, 2317-2324, http://dx.doi.org/10.1016/j.scitotenv.2011.01.057, 2011.
511 Marchuk, A., Marchuk, S.A., Bennett, J.A., Eyres, M.A., Scott, E.: An alternative index to ESP to
512 explain dispersion occurring in Australian soils when Na content is low, National Soils
513 Conference: Proceedings of the 2014 National Soils Conference Soil Science Australia
514 Melbourne, Australia, 2014.
515 Marchuk, A., Rengasamy, P.: Clay behaviour in suspension is related to the ionicity of clay–cation
516 bonds, Appl. Clay Sci., 53, 754-759, http://dx.doi.org/10.1016/j.clay.2011.05.019.
517 Marchuk, S., Marchuk, A.: Effect of applied potassium concentration on clay dispersion, hydraulic
518 conductivity, pore structure and mineralogy of two contrasting Australian soils., Soil Tillage
519 Res., 182, 35-44, http://dx.doi.org/10.1016/j.still.2018.04.016, 2018.
520 Mckenna, B.A., Kopittke, P.M., Macfarlane, D.C., Dalzell, S.A., Menzies, N.W.: Changes in soil
521 chemistry after the application of gypsum and sulfur and irrigation with coal seam water,
522 Geoderma, 337, 782-791, http://dx.doi.org/10.1016/j.geoderma.2018.10.019, 2019.
523 Prajapati, M., Shah, M., Soni, B.: A review of geothermal integrated desalination: A sustainable

524 solution to overcome potential freshwater shortages, J. Clean. Prod., 326, 129412,
525 http://dx.doi.org/10.1016/J.JCLEPRO.2021.129412, 2021.
526 Qadir, M., Oster, J.D., Schubert, S., Noble, A.D., Sahrawat, K.L.: Phytoremediation of Sodic and
527 Saline - Sodic Soils, Adv. Agron., 96, 197-247, http://dx.doi.org/10.1016/S0065-
528 2113(07)96006-X, 2007.
529 Qadir, M., Sposito, G., Smith, C.J., Oster, J.D.: Reassessing irrigation water quality guidelines for
530 sodicity hazard, Agric. Water. Manag., 255, 107054,
531 http://dx.doi.org/10.1016/J.AGWAT.2021.107054, 2021.
532 Reading, L.P., Lockington, D.A., Bristow, K.L., Baumgartl, T.: Are we getting accurate
533 measurements of Ksat for sodic clay soils? Agric. Water. Manag., 158, 120-125,
534 http://dx.doi.org/10.1016/j.agwat.2015.04.015, 2015.
535 Rengasamy, P., Marchuk, A.: Cation ratio of soil structural stability (CROSS), Soil Res., 49, 280-
536 285, http://dx.doi.org/10.1071/SR10105, 2011.
537 Sahin, U., Eroğlu, S., Sahin, F.: Microbial application with gypsum increases the saturated hydraulic
538 conductivity of saline–sodic soils, Appl. Soil Ecol., 48, 247-250,
539 http://dx.doi.org/10.1016/j.apsoil.2011.04.001, 2011.
540 Schjønning, P., Lamandé, M., Berisso, F.E., Simojoki, A., Alakukku, L., Andreasen, R.R.: Gas
541 diffusion, non-darcy air permeability, and computed tomography images of a clay subsoil
542 affected by compaction, Soil Sci. Soc. Am. J., 77, 1977-1990,
543 http://dx.doi.org/10.2136/sssaj2013.06.0224, 2013.
544 Scudiero, E., Skaggs, T.H., Corwin, D.L.: Simplifying field-scale assessment of spatiotemporal

changes of soil salinity, Sci. Total Environ., 587-588, 273-281, http://dx.doi.org/10.1016/j.scitotenv.2017.02.136, 2017.

Shaygan, M., Reading, L.P., Baumgartl, T.: Effect of physical amendments on salt leaching characteristics for reclamation, Geoderma, 292, 96-110, http://dx.doi.org/10.1016/j.geoderma.2017.01.007, 2017.

Singh, G., Mavi, M.S., Choudhary, O.P., Gupta, N., Singh, Y.: Rice straw biochar application to soil irrigated with saline water in a cotton-wheat system improves crop performance and soil functionality in north-west India, J. Environ. Manage., 295, 113277, http://dx.doi.org/10.1016/J.JENVMAN.2021.113277, 2021.

Smiles, D.E., Smith, C.J.: A survey of the cation content of piggery effluents and some consequences of their use to irrigate soils, Soil Res., 42, 231-246, http://dx.doi.org/10.1071/SR03059, 2004.

Smith, C.J., Oster, J.D., Sposito,G.: Potassium and magnesium in irrigation water quality assessment, Agric. Water. Manag., 157, 59-64, http://dx.doi.org/10.1016/j.agwat.2014.09.003, 2015.

Sposito, G., Oster, J.D., Smith, C.J., Assouline, S.: Assessing soil permeability impacts from irrigation with marginal-quality waters, AB Reviews: Perspectives in Agriculture, Veterinary Science, Nutrition and Natural Resources. 11, 15, http://dx.doi.org/10.1079/PAVSNNR201611015, 2016.

Tang, S.Q., She, D.L.: Influence of water quality on soil saturated hydraulic conductivity and infiltration properties, Transactions of the Chinese Society for Agricultural Machinery, 47, 108-114, https://doi.org/10.6041/j.issn.1000-1298.2016.10.015, 2016 (in Chinese).

Tsai, W.T., Liu, S.C., Chen, H.R., Chang, Y.M., Tsai, Y.L.: Textural and chemical properties of

swine-manure-derived biochar pertinent to its potential use as a soil amendment, Chemosphere, 89, 198-203, https://doi.org/10.1016/j.chemosphere.2012.05.085, 2012.

Vaezi, A.R., Ahmadi, M., Cerdà, A.: Contribution of raindrop impact to the change of soil physical properties and water erosion under semi-arid rainfalls, Sci. Total Environ., 583, 382-392, http://dx.doi.org/10.1016/j.scitotenv.2017.01.078, 2017.

Weiler, M., Naef, F.: Simulating surface and subsurface initiation of macropore flow, J. Hydrol., 273, 139-154, http://dx.doi.org/10.1016/S0022-1694(02)00361-X, 2003.

Wilson, G.V., Luxmoore, R.J.: Infiltration, macroporosity, and mesoporosity distributions on two forested watersheds, Soil Sci. Soc. Am. J., 52, 329-335, http://dx.doi.org/10.2136/sssaj1988.03615995005200020005x, 1988.

Xu, J., Huang, P.M.: Soil Science, China Agriculture Press, Beijing, China, 2010 (in Chinese).

Yang, G., Li, F., Tian, L., He, X., Gao, Y., Wang, Z., Ren, F.: Soil physicochemical properties and cotton (Gossypium hirsutum L.) yield under brackish water mulched drip irrigation, Soil Tillage Res., 199, 104592, https://doi.org/10.1016/j.still.2020.104592, 2020.

Yin, C.Y., Zhao, J., Chen, X.B., Li, L.J., Liu, H., Hu, Q.L.: Desalination characteristics and efficiency of high saline soil leached by brackish water and Yellow River water, Agric. Water. Manag., 263, 107461, http://dx.doi.org/10.1016/J.AGWAT.2022.107461, 2022.

Yu, Z.H., Liu, X.M., Xu, C.Y., Xiong, H.L., Li, H.: Specific ion effects on soil water movement, Soil Tillage Res., 161, 63-70, http://dx.doi.org/10.1016/j.still.2016.03.004, 2016.

Zhang, H.X., Xie, Y.Z.: Alleviating freshwater shortages with combined desert-based large-scale renewable energy and coastal desalination plants supported by Global Energy Interconnection,

Glob. Energy Interconnec., 2, 205-213, http://dx.doi.org/10.1016/j.gloei.2019.07.013, 2019.

Zhang, T.B., Zhan, X.Y., He, J.Q., Feng, H., Kang, Y.H.: Salt characteristics and soluble cations redistribution in an impermeable calcareous saline-sodic soil reclaimed with an improved drip irrigation, Agric. Water. Manag., 197, 91-99, https://doi.org/10.1016/j.agwat.2017.11.020, 2018.

Zhu, Y., Bennett, J.M., Marchuk, A.: Reduction of hydraulic conductivity and loss of organic carbon in non-dispersive soils of different clay mineralogy is related to magnesium induced disaggregation, Geoderma, 349, 1-10, https://doi.org/10.1016/j.agwat.2017.11.020, 2019.